Novel Pyridine-Based Poly(ether sulfones) and their Study in High Temperature PEM Fuel Cells

M. Georgezi,[†,‡,§] V. Deimede,[§] N. Gourdoupi,[§] N. Triantafyllopoulos,[§] S. Neophytides,*[,‡,§] and J. K. Kallitsis*[,†,‡,§]

Department of Chemistry, University of Patras, GR-26500 Rio-Patras, Greece, Institute of Chemical Engineering and High Temperature Chemical Processes, ICE/HT-FORTH, Post Office Box 1414, GR-26504 Rio-Patras, Greece, and Advent Technologies SA, Patras Science Park, GR-26504 Rio-Patras, Greece

Received July 24, 2008; Revised Manuscript Received October 10, 2008

ABSTRACT: Novel pyridine-based aromatic copolymers containing 4,4′-biphenol or hydroquinone groups in the main chain were synthesized and characterized as polymer electrolytes for proton exchange membrane fuel cells (PEMFCs). Depending on the copolymer composition and pyridine monomer content in most cases soluble and high molecular weight copolymers were obtained. Flexible membrane films were prepared by casting *N*,*N*-dimethylacetamide (DMA_C) solutions of copolymers. ^1H NMR and size exclusion chromatography were used to characterize the structures of the copolymers. High glass transition temperatures (T_gs) and decomposition temperatures (T_ds) were observed using dynamic mechanical analysis and thermogravimetry, respectively. The oxidative stability of the membranes was examined with Fenton′s test. The doping ability and the proton conductivity of the membranes were also studied and the new copolymers can be potential candidates as new polymeric electrolyte materials for proton exchange membrane fuel cells. Finally, membrane electrode assemblies (MEAs) were constructed and tested in 25 cm^2 single cell at different temperatures showing promising performance.

1. Introduction

The proton exchange membrane fuel cells (PEMFCs) are advanced power systems that can cover in a sustainable way the future energy demands. They are highly energy efficient, clean, and environmentally friendly.[1] Because of their potential to reduce dependence on fossil fuels and diminish poisonous emissions into the atmosphere, PEMFCs have emerged as alternative to combustion engines. PEMFCs use pure hydrogen as fuel, which is an excellent energy carrier and can be produced from different renewable energy sources like solar, hydro, biomass, wind, geothermal, and so on.[2] The only product is water, thus rendering these systems the most clean energy technology.[3] In the mean time and because hydrogen obtained from reformation of fossil fuels or biofuels is available, the presence of few percent carbon monoxide is the key problem and can be overcome by using fuel cells operating at higher temperatures.

In a PEMFC, the proton exchange membrane (PEM) is the core part of the cell. The prerequisites in primary properties[4] for a polymeric membrane to be used in a PEMFC are high proton conductivity, low electronic conductivity, good mechanical properties, oxidative and chemical integrity, low permeability to gases, and limited swelling in the presence of water. It is also imperative to have low cost and being capable for fabrication into MEAs.

Membranes commonly used in PEMFC are perfluorinated polymers containing sulfonic acid groups on side chains, like for example Nafion,[5] manufactured by DuPont. Such membranes suffer from high cost, low operating temperature, and hydrogen permeability. As a result, they exhibit good performance only at moderate temperatures (less than 90 °C) and high humidity using pure hydrogen gas as fuel. The operation of a PEMFC at elevated temperatures has the benefits of reducing CO poisoning of platinum electrocatalyst and increasing reaction kinetics.[6] That is why so much effort is presently devoted to the development of alternative polymeric membranes able to stand higher temperatures. In this respect, new polymeric materials based on aromatic backbones have recently been synthesized. Potential polymers[7] for this aim include polyethersulfones, polyetherketones, polyimides, and polybenzimidazoles.

Savinell et al.[8] proposed that polybenzimidazole (PBI) can be used as a high temperature polymer electrolyte after doping with strong acids[9] such as phosphoric acid or sulfuric acid. However, PBI presents moderate mechanical properties and low oxidative stability. These drawbacks in combination with the limited availability and its high cost have stimulated a research effort for the development of different polybenzimidazole structures,[10] nafion-polybenzimidazole blends[11] or alternative polymeric materials.[12] Nowadays, poly(2,5-benzimidazole) (AB-PBI), the simplest polybenzimidazole type polymer, exhibits comparable thermal and conductance properties as that of PBI and because of the fact that it does not contain the phenylene ring in the polymer backbone, leads to higher acid uptake[13] in comparison with commercial PBI. Synthesis and fuel cell performance of ABPBI is already reported in the literature.[14] However, the fact that this material is soluble only in strong acids makes its process to final doped membranes difficult and need further improvement.

Alternative polymeric structures that have been able to give membranes for high temperature fuel cells were produced by our group.[15] These materials combine excellent mechanical and oxidative stability with the ability to absorb strong protic acids giving ionically conductive membranes. Because the challenge is to combine solubility of high molecular weight aromatic polymers with high thermal transition properties, a lot of synthetic effort is needed to find the best materials. This is mainly due to the inherent insolubility problems that arise from the structural rigidity, which is necessary to ensure the exceptional mechanical and thermal properties.

* To whom correspondence should be addressed. Phone: (+30)2610-997121(J.K.K.); (+30)2610-965265(S.N.). Fax: (+30)2610-997122 (J.K.K.). E-mail: j.kallitsis@chemistry.upatras.gr (J.K.K.); neoph@iceht.forth.gr (S.N.).
† University of Patras.
‡ ICE/HT-FORTH.
§ Advent Technologies SA.

10.1021/ma801678h CCC: $40.75
Published on Web 11/11/2008

Our approach is here extended to the synthesis of copolymers containing basic groups that give high molecular weight soluble polymers without the use of any solubilizing group and at the same time have the ability to form complexes with strong acids. More specifically, in this work, we report the synthesis of new soluble aromatic poly(ether sulfone) copolymers containing pyridine and 4,4′-biphenol or hydroquinone to develop alternative polymer electrolytes for high temperature use. Synthesis of new copolymers having a rigid aromatic polyether backbone and polar groups like the pyridine ring results in materials with thermal and chemical stability and high ionic conductivity after doping with phosphoric acid. Based on these membranes, new membrane electrode assemblies (MEAs) were constructed and were tested under real fuel cell conditions at temperatures up to 180 °C showing promising performance.

2. Experimental Section

2.1. Materials and Instrumentation. 2,5-Bis(4-hydroxyphenyl)pyridine was prepared according to literature procedure,[15a] while bis(4-fluorophenyl)-sulfone, 4,4′-biphenol and hydroquinone were obtained from Aldrich. Solvents were purchased from Aldrich and were used without further purification. For the materials used in electrode construction, carbon cloth supporting layer and catalyst powder (30 wt % Pt/Vulcan XC-72R) were purchased from E-Tek Inc. (BASF Fuel Cell Division), SAB carbon powder was purchased from Cabot Inc. and PTFE dispersion in water from Aldrich. ^{1}H NMR spectra were obtained on a Brucker Advance DPX 400 MHz spectrometer with deuterated $CDCl_3$. Gel permeation chromatography (GPC) measurements were carried out using a Polymer Laboratory chromatographer equipped with two Ultra Styragel Columns (10^4, 500 Å), UV detector (254 nm), and $CHCl_3$ as eluent with polystyrene standards for calibration. Dynamic mechanical analysis (DMA) measurements were performed using a solid-state analyzer RSA II, Rheometrics Scientific Ltd. at 10 Hz. Thermogravimetric analysis (TGA) was carried out by a DuPont 990 thermal analyzer coupled to a DuPont 951 TGA accessory. Conductivity measurements were conducted by the four-probe current interruption method using a potentiostat/galvanostat (EG and G model 273) and an oscillator (Hitachi model V-650F). Electrochemical characterization was carried out using the potentiostat/galvanostat Autolab PGSTAT30 equipped with the Booster20A (Eco Chemie).

2.2. Synthesis of Poly(ether sulfones) Copolymers Containing 4,4′-Biphenol or Hydroquinone Groups in the Main Chain. A typical polymerization procedure is as follows. To a degassed flask equipped with a Dean−Stark trap were added 2,5-bis(4-hydroxyphenyl)pyridine, bis(4-fluorophenyl)-sulfone, 4,4′-biphenol, or hydroquinone, potassium carbonate, dimethylformamide, and toluene. The mixture was degassed under argon and stirred at 150 °C for 24 h and then stirred at 180 °C for about 6 h. The viscous product was diluted in dimethylformamide and precipitated in a 10-fold excess mixture of 2/1 methanol/water, washed with water and hexane, and dried at 80 °C under vacuum for 1 day. The same procedure was followed to produce copolymers with different pyridine monomer content and thus different copolymer composition. The results in terms of copolymer composition and molecular weight characteristics are shown in Table 1.

Example for the Synthesis of Poly(ether sulfones) Copolymers Containing 4,4′-Biphenol Groups in the Main Chain is Given for Copolymer I_c. 2,5-Bis(4-hydroxyphenyl)pyridine 0.4138 g (1.57 mmol), 4,4′-biphenol 0.2930 g (1.57 mmol), bis(4-fluorophenyl)-sulfone 0.8000 g (3.15 mmol), potassium carbonate 0.5037 g (3.65 mmol), dimethylformamide 10 mL, and toluene 6 mL were added to a degassed flask equipped with a Dean−Stark trap and the mixture was polymerized according the above-described procedure.

Example for the Synthesis of Poly(ether sulfones) Copolymers Containing Hydroquinone Groups in the Main Chain is Given for Copolymer II_b. 2,5-Bis(4-hydroxyphenyl)pyridine 0.4138 g (1.57 mmol), hydroquinone 0.1732 g (1.57 mmol), bis(4-fluorophenyl)-sulfone 0.8000 g (3.15 mmol), potassium carbonate 0.5037 g (3.65 mmol), dimethylformamide 10 mL, and toluene 6 mL were added to a degassed flask equipped with a Dean−Stark trap and polymerized as described above.

Table 1. Gel Permeation Chromatography of the Synthesized Copolymers

copolymer	x	M_n	M_w	disp
I_a	0.5	27000	53000	2.0
I_b	0.5	34000	54000	1.6
I_c	0.5	44000	71000	1.6
I_d	0.6	28000	42000	1.5
I_e	0.6	30000	48000	1.6
I_f.	0.6	38000	64000	1.7
II_a	0.5	67000	112000	1.7
II_b	0.5	89000	136000	1.5
II_c	0.5	93000	143000	1.5
II_d	0.5	115000	172000	1.5
II_e	0.6	93000	154000	1.7
II_f	0.6	112000	178000	1.6
II_g	0.7	61000	96000	1.6
II_h	0.7	86000	150000	1.7
II_i	0.75	63000	132000	2.1
II_j	0.75	72000	120000	1.7

2.3. Membrane Preparation. The copolymers were dissolved in dimethylacetamide at room temperature. The solutions of the different copolymers were cast on glass plates and the solvent slowly evaporated at 80 °C. The resulting membranes were dried under vacuum at 160 °C for 3 days. The drying procedure was optimized to produce flat, transparent membranes while quantitatively removing the casting solvent.

2.4. Doping Procedure. The membranes were immersed into 85 wt % phosphoric acid solution at various temperatures and doping times to obtain the maximum doping level. The wet membranes were wiped, dried, and quickly weighed on an analytical balance until a constant acid uptake was obtained. The acid uptake of membranes is reported as a percentage and is determined as follows

$$\text{acid uptake} = (W_{\text{wet}} - W_{\text{dry}}) \times 100 / W_{\text{dry}} \quad (1)$$

where W_{wet} and W_{dry} are the weights of the wet and dry membranes, respectively.

2.5. Fenton's Test. Thin membrane samples were immersed into 3% H_2O_2 aqueous solution containing 4 ppm $FeCI_24H_2O$ at 80 °C for 72 h.[16] Both thermal and mechanical properties of the dried samples before and after the experiment were compared. The oxidative stability of the samples was examined with dynamic mechanical analysis and thermogravimetric analysis.

2.6. Conductivity Measurements. The initial electrochemical characterization of the acid-doped membranes was carried out using the four probe current interruption method.[17] The dependence of the ionic conductivity on temperature for high doping levels was examined as well as the dependence of the ionic conductivity versus doping level.

2.7. Electrodes Preparation and MEA Fabrication. The handmade electrodes were prepared from ink by mixing the catalyst powder (30 wt % Pt/C, E-Tek Inc. BASF Fuel Cell Division), the desired amount of polymeric binder and *N*,*N*-dimethylacetamide (DMAc) as solvent, on a gas diffusion layer (GDL). GDL was homemade using carbon cloth from E-Tek Inc. (BASF Fuel Cell Division) on which was sprayed slurry made of SAB carbon and PTFE dispersion, followed by sintering at 300 °C under static air for 40 min. Finally, the electrodes were treated for 12 h at 80 °C and 3 d at 190 °C under vacuum in order to remove the organic solvent. MEAs were fabricated by placing the electrodes on both sides of the phosphoric acid doped membrane (doping level ~ 220 wt %) and then hot pressing at 150 °C for 15 min. In this work, the cathode side and the anode side use the same electrodes with catalyst loading 0.9 mg/cm^2, while the assembling force for the single cell was 4 Nm or 0.1 t/cm^2.

2.8. Electrochemical Characterization. The electrochemical evaluation of the MEAs (with 25 cm^2 active area) was carried out in a single cell with serpentine flow channels (Fuel Cell Technolo-

Scheme 1. Synthesis of Pyridine Based Poly(ethersulfones)

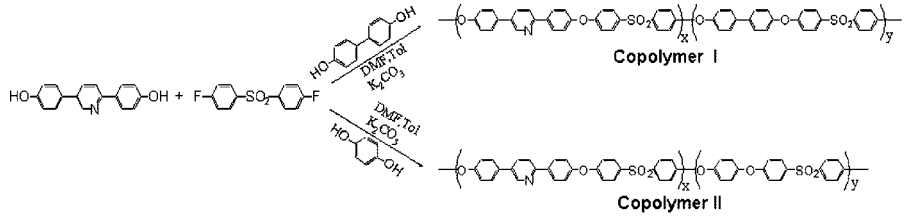

gies Inc.). Pure hydrogen and oxygen gases were supplied to the anode and cathode compartments, respectively. A constant reactant utilization of 67% for oxygen and 83% for hydrogen were used. All measurements were performed within the temperature range of 140−180 °C at ambient pressure. Polarization curves were recorded at different temperatures using the potentiostat/galvanostat PGSTAT30. The steady state current was being recorded for 30 s after each potential was set. The electrochemical impedance spectra (EIS) were recorded at 0.5 V in the frequency range of 10 mHz to 20 kHz with an amplitude of sinusoidal signal of 10 mV rms, using the same equipment. All measurements reported in this paper were made in two-electrode arrangement, with the anode serving as both counter and reference electrode and the cathode used as working electrode.

3. Results and Discussion

As was mentioned in the introduction in cases that aromatic rigid polymers are the materials of choice for an application, the key problem is to find the proper way to ensure the preparation of high molecular weight polymers that combine solubility with any additional desired specific function. In the case of polymer electrolytes for high temperature fuel cells the additional property is the ionic conductivity which is realized by the ability of the polymer electrolyte to be doped with strong acids and also to keep this acid content under the operation conditions. In this work we were able to synthesize such materials based on aromatic polyether copolymers having high molecular weight, in some cases exceeding 100000 (M_n value) but still keeping the solubility, giving high quality films that additionally were able to be doped with phosphoric acid reaching high doping values. This was realized without disturbing the para-aromatic character by using the copolymerization approach where diols of different rigidity were used to disturb the structure regularity and subsequently the extent of the intermolecular interactions that are mainly responsible for the insolubility problems. Thus, our present approach toward the development of new polymeric materials for use in high temperature PEMFCs is based on the incorporation of polar pyridine groups in polymeric backbones of aromatic polyethers.[15]

High temperature nucleophilic substitution polycondensation of bis(4-fluorophenyl)-sulfone with 2,5-bis(4-hydroxyphenyl)-pyridine and hydroquinone or biphenol diols by varying copolymerization times, temperatures and ratios of the two diols resulted in new aromatic copolymers with excellent film forming properties (Scheme 1).

High molecular weights were obtained in all cases as proven by size exclusion chromatography characterization with PS standards as depicted in Table 1.

An example of ^{1}H NMR spectrum, supporting the structure of copolymer II_b, is given in Figure 1. The spectrum for the copolymer II_b shows a ratio of the integration of the peak at 8.92 ppm, which is due to the 'a' hydrogen of the 2,5-bis(4-hydroxyphenyl)pyridine unit, to the peak at 7.18 ppm, which is attributed to the "h" hydrogens of the bis(4-fluorophenyl)-sulfone, equal to 1/4, as expected for this structure.

To explore to what extent the copolymers can keep the solubility and taking into account that the homopolymer composed of the 2,5-bis(4-hydroxyphenyl)pyridine and bis(4-fluorophenyl)-sulfone is insoluble, we synthesized copolymers with various pyridine contents as shown in Table 1. Copolymers I with 50 mol % of the 2,5-bis(4-hydroxyphenyl)pyridine and 50 mol % of the 4,4′-biphenol (copolymers I_a-I_c) were synthesized resulting in MWs, which range from 27000−44000. Copolymers I with 60 mol % of the 2,5-bis(4-hydroxyphenyl)pyridine diol (copolymers I_d-I_f) were synthesized to test the limits in acid uptake. However, low molecular weight copolymers were obtained and it must be due to their insolubility. To improve solubility properties we synthesized high molecular weight copolymers with MWs values in the range of 61000−115000 in the case that hydroquinone which has one less aromatic ring was used instead of 4,4′-biphenol. Copolymers II with 50 mol % and 60 mol % of the 2,5-bis(4-hydroxyphenyl)pyridine diol (copolymers II_a-II_f) were synthesized and showed good solubility in common organic solvents, while in the case of copolymers II with 70 mol % and 75 mol % of the 2,5-bis(4-hydroxyphenyl)pyridine diol (copolymers II_g-II_j), the copolymers were partially soluble.

Dynamic mechanical analysis (DMA) was used to examine the mechanical properties of the copolymers I_c, II_b, and II_e. As presented in Figure 2, all used copolymers exhibit glass transition temperature in the range of 230−245 °C depending on the structure and the copolymer composition. Comparing the two different copolymer structures (copolymers I_c and II_b) with the same 2,5-bis(4-hydroxyphenyl)pyridine monomer content, an increase in the glass transition temperature was observed as 4,4′-biphenol diol was used instead of hydroquinone diol due to the more rigid backbone of the copolymer I_c. Regarding the same copolymers structures (copolymers II_b and II_e), an increase in the glass transition temperature was observed as the 2,5-bis(4-hydroxyphenyl)pyridine monomer percentage increases.

The doping behavior with 85 wt % phosphoric acid at several doping temperatures and times was studied in order to evaluate the potential of these copolymers for further use in single cells. The copolymers II_b and II_e exhibit higher doping ability than copolymer I_c possibly because of their more flexible structrure (II_b and II_e copolymers have phenylene main chain entities compared to biphenylene in the case of copolymer I_c). Thus, at

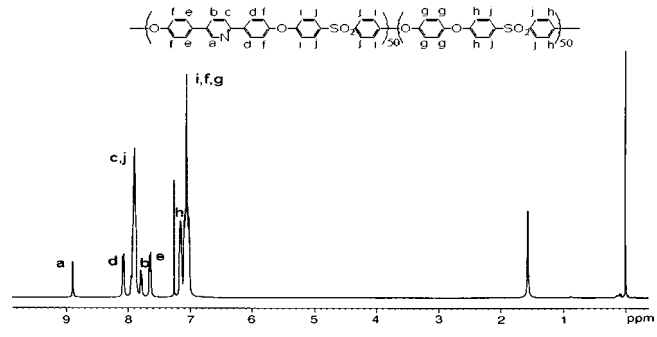

Figure 1. ^{1}H NMR spectrum with the assessment of the peaks of the copolymer II_b.

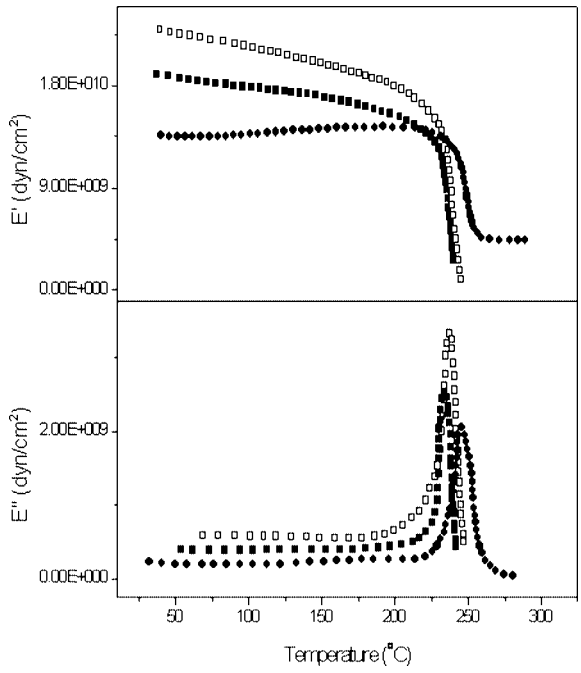

Figure 2. Temperature dependence of the storage (E') and loss (E'') modulus for copolymers I_c (●), II_b (■) and II_e (□).

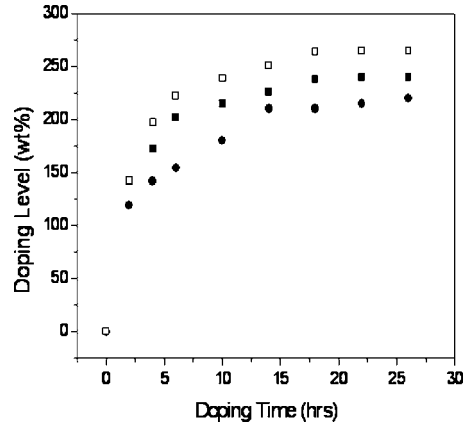

Figure 3. Time dependence of doping level (wt %) of copolymers I_c (●), II_b (■) and II_e (□), respectively.

120 °C, copolymers II_b and II_e reach their maximum doping level of 240 wt % and 265 wt %, respectively, as shown in Figure 3. Additionally, in the case of copolymers II_b and II_e, an increase in the acid uptake was obtained as the 2,5-bis(4-hydroxyphenyl)pyridine monomer percentage increases.

The chemical, thermal, and oxidative stability of the copolymer II_b which presents better solubility as compared to copolymer II_e and higher acid uptake as compared to copolymer I_c was tested using the Fenton's test. More specifically, the oxidative stability of copolymer II_b, after treatment with the Fenton reagent, was examined with dynamic mechanical analysis and thermogravimetric analysis as shown in Figures 4 and 5. The membrane samples retained their mechanical integrity as well as their thermal stability up to 470 °C. Moreover and to exclude any structural change, size exclusion chromatography characterization and ^{1}H NMR spectroscopy were performed before and after Fenton's test. It was observed that the treated membranes retain their solubility properties showing no detectable structural changes, supporting thus the high oxidative stability of these materials.

A sample of copolymer II_b doped with phosphoric acid was also selected in order to evaluate the doping dependence of the

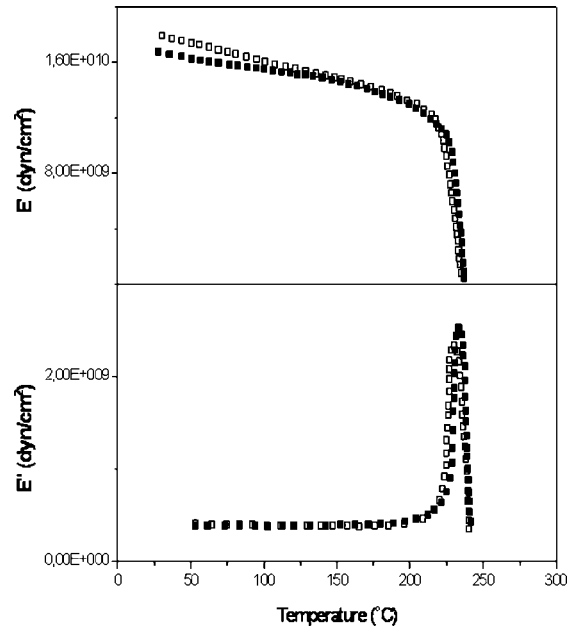

Figure 4. Temperature dependence of the storage (E') and loss (E'') modulus for copolymer II_b before (■) and after (□) the treatment with H_2O_2.

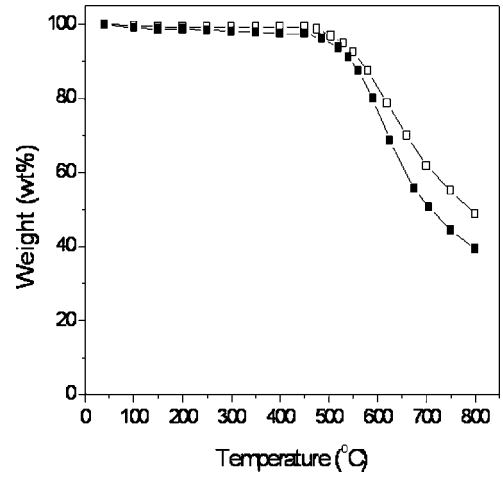

Figure 5. Thermogravimetric analysis for copolymer II_b before (■) and after (□) the treatment with H_2O_2.

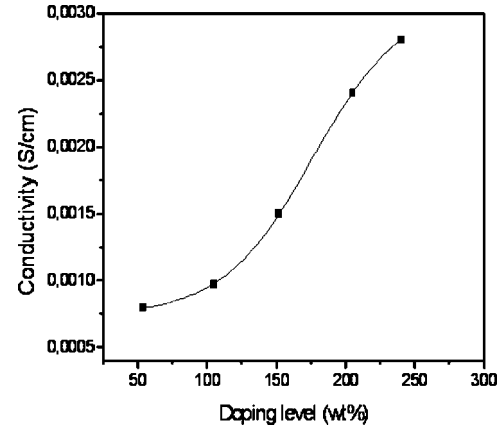

Figure 6. Doping level dependence of ionic conductivity of copolymer II_b at room temperature.

conductivity as shown in Figure 6. Moreover, a sample of copolymer II_b doped with 240 wt % phosphoric acid was also

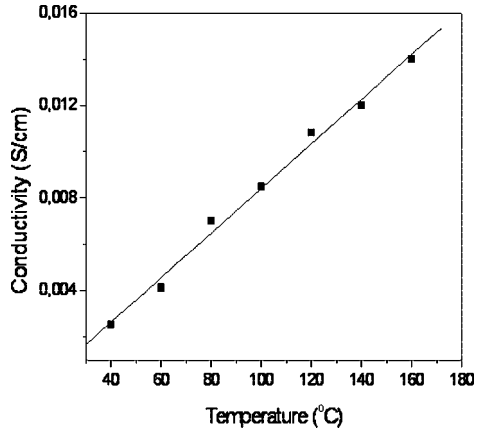

Figure 7. Temperature dependence of ionic conductivity of acid doped copolymer II_b with a doping level 240 wt % H_3PO_4.

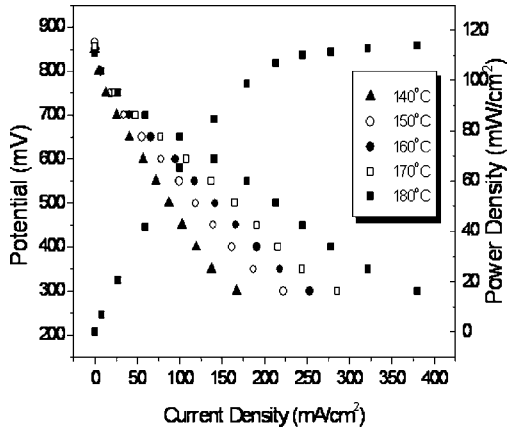

Figure 8. Polarization curves for the copolymer II_b at several temperatures between 140−180 °C. Hydrogen: 1.2 × stoichiometry, ambient pressure, and 0% RH. Oxygen: 1.5 × stoichiometry, ambient pressure, and 0% RH.

selected to evaluate the temperature dependence of the conductivity as shown in Figure 7. Conductivity increases as doping level and temperature increase and values in the range of 10^{-2} S/cm were obtained at temperatures higher than 120 °C. Since higher doping level values were obtained with these polymeric structures one should expect that compared to analogous polymers, copolymers and blends[15] with lower doping level, the conductivity values should be higher. However, it does not happen in all cases and this is a strong indication that not only the doping level, but the whole polymeric matrix, plays a role in the final ionic conductivity of the membrane. Furthermore the temperature dependence of the conductivity for copolymer II_b shows high conductivity values of 1.4×10^{-2} S/cm for 240 wt % doping level at 160 °C. This is mainly attributed to the polymeric chain morphology because in these copolymers there are no steric reasons that could hinder the proton transport.

The copolymer II_b was selected to be tested in a 25 cm^2 single cell with the initial phosphoric acid doping level of the membrane at 220 wt % and the Pt loading on the electrodes at 0.9 mg/cm^2. Figure 8 illustrates the polarization curves of the fuel cell at several operating temperatures between 140 and 180 °C using dry gases with anode and cathode stoichiometric ratio of 1.2 and 1.5, respectively, at ambient pressure. These curves indicate that the fuel cell performance was improved with increasing temperatures from 140 to 180 °C, which can be explained by the increase in the membrane conductivity at higher temperatures as already has been depicted in Figure 7. The maximum performance is observed at 180 °C with a current density of 214 mA/cm^2 at cell voltage of 0.5V. This performance

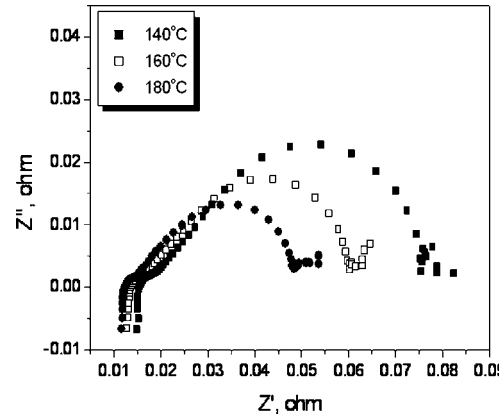

Figure 9. Nyquist plot for the copolymer II_b as a function of temperature. Hydrogen: 1.2 × stoichiometry, ambient pressure, and 0% RH. Oxygen: 1.5 × stoichiometry, ambient pressure, and 0% RH.

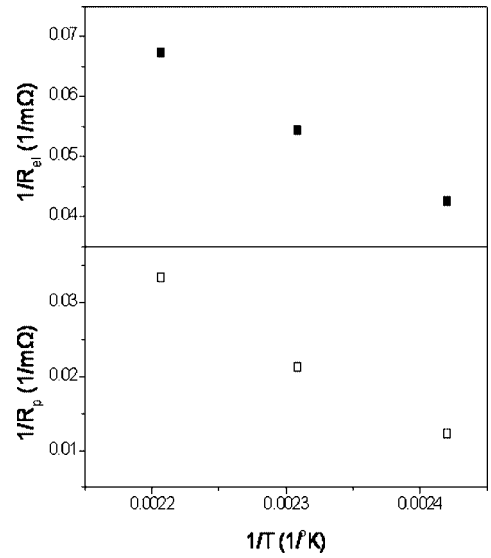

Figure 10. Ohmic and polarization resistance for the copolymer II_b as a function of temperature. Hydrogen: 1.2 × stoichiometry, ambient pressure, and 0% RH. Oxygen: 1.5 × stoichiometry, ambient pressure, and 0% RH.

may be considered not high one, but it should be noted that no optimization regarding the MEA has been performed so far. This is clearly shown by the AC impedance measurements depicted as Nyquist plots on a complex plane in Figure 9 at different temperatures during fuel cell operation at 0.5 V. The real Z-axis intercept at high frequency provides mainly the electrolyte resistance (R_{el}) and, hence, its conductivity. The difference between the low and high frequency intercepts is used for the determination of the electrokinetic (polarization) resistance of the electrochemical interfaces. As it is depicted in Figure 9 and 10 both ionic resistance and electrokinetic resistance decrease with increasing temperature. Nevertheless the polarization resistance is mostly affected by temperature thus denoting that the improvement of the electrocatalytic activity of the electrode/electrolyte interface is of vital importance for the optimization of the MEAs performance.

4. Conclusions

New pyridine-based wholly aromatic polyether copolymers containing 4,4′-biphenol or hydroquinone were synthesized and characterized as polymer electrolytes for proton exchange membrane fuel cells (PEMFCs). Most of the studied copolymers

exhibit good mechanical properties, excellent film forming properties and high oxidative and thermal stability. The membranes prepared from these copolymers, are easily doped with phosphoric acid showing high acid uptake which is affected from the detailed polymeric structure and not only from the pyridine content in the main chain. Ionic conductivities in the range of 10^{-2} S/cm were obtained for these membranes after doping with phosphoric acid. Additional information of the influence of the polymeric structure on the conductivity, was obtained by comparing these materials with the ones previously studied.[15] Furthermore, the copolymer II_b was selected to be tested in a 25 cm^2 single cell operating to temperatures up to 180 °C.

At a cell voltage of 0.5 V, a current density of 214 mA/cm^2 was obtained with H_2/O_2 at 180 °C without external humidification. This initial single cell test showed promising results, through an optimization of different parameters involving the MEAs construction and the single cell operation conditions.

Acknowledgment. Partial financial support of the EPAN E-25 project and APOLLON B European Project (Contract No. 33228) is gratefully acknowledged. EPAN E-25 project is cofunded: 75% of public financing from the European Union-European Social Fund and 25% of public financing from the Greek State-Ministry of Development-GSRT in the framework of the Operational Program "Competitiveness"-Measure 4.5.1, Community Support Framework 2000−2006.

References and Notes

(1) (a) Dresselhaus, M. S.; Thomas, I. L. *Nature* **2001**, *414*, 332–337. (b) Borup, R.; Meyers, J.; Pivovar, B.; Kim, Y. S.; Mukundan, R.; Garland, N.; Myers, D.; Wilson, M.; Garzon, F.; Wood, D.; Zelenay, P.; More, K.; Stroh, K.; Zawodzinski, T.; Boncella, J.; McGrath, J. E.; Inaba, M.; Miyatake, K.; Hori, M.; Ota, K.; Ogumi, Z.; Miyata, S.; Nishikata, A.; Siroma, Z.; Uchimoto, Y.; Yasuda, K.; Kimijima, K.-I.; Iwashita, N. *Chem. Rev.* **2007**, *107*, 3904–3951.

(2) (a) Johnston, B.; Mayo, M. C.; Khare, A. *Technovation* **2005**, *25*, 569–585. (b) Sherif, S. A.; Barbir, F.; Veziroglou, T. N. *Solar Energy* **2005**, *78*, 647–660.

(3) Sopian, K.; Daud, W. R. W. *Renewable Energy* **2006**, *31*, 719–727.

(4) (a) Hickner, M. A.; Ghassemi, H.; Kim, Y. S.; Einsla, B. R.; McGrath, J. E. *Chem. Rev.* **2004**, *104*, 4587–4612. (b) Smitha, B.; Sridhar, S.; Khan, A. A. *J. Membr. Sci.* **2005**, *259*, 10–26.

(5) Mauritz, K. A.; Moore, R. B. *Chem. Rev.* **2004**, *104*, 4535–4585.

(6) Zhang, J.; Xie, Z.; Zhang, J.; Tang, Y.; Song, C.; Navessin, T.; Shi, Z.; Song, D.; Wang, H.; Wilkinson, D. P.; Liu, Z.-S.; Holdcroft, S. *J. Power Sources* **2006**, *160*, 872–891.

(7) (a) Kerres, J. A. *J. Membr. Sci.* **2001**, *185*, 3–27. (b) Roziere, J.; Jones, D. J. *Annu. Rev. Mater. Res.* **2003**, *33*, 503–555. (c) Qingfeng, L.; He, R.; Jensen, J. O.; Bjerrum, N. J. *Chem. Mater.* **2003**, *15*, 4896–4915. (d) Krishnan, N. N.; Kim, H.-J.; Prasanna, M.; Cho, E.; Shin, E.-M.; Lee, S.-Y.; Oh, I.-H.; Hong, S.-A.; Lim, T.-H. *J. Power Sources* **2006**, *158*, 1246–1250. (e) Wang, Z.; Li, X.; Zhao, C.; Ni, H.; Na, H. *J. Power Sources* **2006**, *160*, 969–976.

(8) (a) Wainright, J. S.; Wang, J. T.; Weng, D.; Savinell, R. F.; Litt, M. H. *J. Electrochem. Soc.* **1995**, *142*, L121–L123. (b) Samms, S. R.; Wasmus, S.; Savinell, R. F. *J. Electrochem. Soc.* **1996**, *143*, 1225–1232.

(9) (a) Ma, Y. L.; Wainright, J. S.; Litt, M. H.; Savinell, R. F. *J. Electrochem. Soc.* **2004**, *151* (1), A8–A16. (b) Bouchet, R.; Siebert, E. *Solid State Ionics* **1999**, *118*, 287–299. (c) Kawahara, M.; Morita, J.; Rikukawa, M.; Sanui, K.; Ogata, N. *Electrochim. Acta* **2000**, *45*, 1395–1398.

(10) (a) Carollo, A.; Quartarone, E.; Tomasi, C.; Mustarelli, P.; Belotti, F.; Magistris, A.; Maestroni, F.; Parachini, M.; Garlaschelli, L.; Righetti, P. P. *J. Power Sources* **2006**, *160*, 175–180. (b) Xiao, L.; Zhang, H.; Jana, T.; Scanlon, E.; Chen, R.; Choe, E.-W.; Ramanathan, L. S.; Yu, S.; Benicewicz, B. C. *Fuel Cells* **2005**, *5*, 287–295.

(11) Wycisk, R.; Chisholm, J.; Lee, J.; Lin, J.; Pintauro, P. N. *J. Power Sources* **2006**, *163*, 9–17.

(12) (a) Wang, F.; Hickner, M.; Kim, Y. S.; Zawodzinski, T. A.; McGrath, J. E. *J. Membr. Sci.* **2002**, *197*, 231–242. (b) Harrison, W. L.; Wang, F.; Mecham, J. B.; Bhanu, V. A.; Hill, M.; Kim, Y. S.; McGrath, J. E. *J. Polym. Sci., Part A: Polym. Chem.* **2003**, *41*, 2264–2276.

(13) Asensio, J. A.; Gomez-Romero, P. *Fuel Cells* **2005**, *5*, 336–342.

(14) (a) Kim, H. J.; Cho, S. Y.; An, S. J.; Eun, Y. C.; Kim, J. Y.; Yoon, H. K.; Kweon, H. J.; Yew, K. H. *Macromol. Rapid Commun.* **2004**, *25*, 894–897. (b) Asensio, J. A.; Borros, S.; Gomez-Romero, P. *Electrochem. Commun.* **2003**, *5*, 967–972. (c) Asensio, J. A.; Borros, S.; Gomez-Romero, P. *J. Membr. Sci.* **2004**, *241*, 89–93.

(15) (a) Gourdoupi, N.; Andreopoulou, A. K.; Deimede, V.; Kallitsis, J. K. *Chem. Mater.* **2003**, *15*, 5044–5050. (b) Pefkianakis, E. K.; Deimede, V.; Daletou, M. K.; Gourdoupi, N.; Kallitsis, J. K. *Macromol. Rapid Commun.* **2005**, *26*, 1724–1728. (c) Daletou, M. K.; Gourdoupi, N.; Kallitsis, J. K. *J. Membr. Sci.* **2005**, *252*, 115–122.

(16) (a) Kosmala, B.; Schauer, J. *J. Appl. Polym. Sci.* **2002**, *85*, 1118–1127. (b) Hubner, G.; Roduner, E. *J. Mater. Chem.* **1999**, *9*, 409–418. (c) Gourdoupi, N.; Papadimitriou, K.; Neophytides, S.; Kallitsis, J. K. *Fuel Cells* **2008**, *8*, 200–208.

(17) Hasiotis, C.; Qingfeng, L.; Deimede, V.; Kallitsis, J. K.; Kontoyannis, C. G.; Bjerrum, N. G. *J. Electrochem. Soc.* **2001**, *148*, A513–A519.

MA801678H